

The Impact-Triggered Flash Cascade (ITFC) Model and a Rotation-Based Interpretation of Particle Motion — Draft v0.1

> Corresponding author: Koh, Hyun-Kyu

Co-author: Tendo Aris

Abstract

We propose the **Impact- Triggered Flash Cascade (ITFC)** model, which interprets visible light as a cascade of flashes emitted by an unobservable background of particles (U- particles) excited through contact with a high- speed driver (P- particle). In this framework the observable signal is not the P- particle itself but the propagation of the **U- cascade**. The speed constant **C** is not the speed of P; rather, it is the **critical rotational- transfer speed of U**. While a P- particle may satisfy $v_p \geq c$ (*a lower bound*), information transfer is limited by the cascade propagation speed $v_{eff} \leq c$, preserving local relativistic invariance. U- cascade propagation is governed by two phenomenological parameters—the effective transfer length λ and the local dwell/lag time τ_e —from which we obtain

$$v_{eff} = \frac{1}{c^{-1} + \tau_e/\lambda}, \quad n = 1 + \frac{c\tau_e}{\lambda}$$

1. Introduction

Scope notice. This paper focuses on phenomenology: we formalize optical consequences in terms of λ , τ_e , \mathcal{K} without committing to a full microscopic model. A concrete definition of U- particles, their creation/interaction rules, a rotation- field- based dynamics, and a mapping to standard field theory will be presented **in subsequent papers**.

Conventional optics treats light via Maxwell's equations and quantum electrodynamics. Here

we examine whether a **contact-transfer mechanical micro-picture** can reproduce macroscopic optical laws while remaining compatible with relativistic constraints. The central idea is: space is filled with unobservable background particles (U); impact by a high-speed driver (P) excites U into a transient, rapidly rotating state (**U***), which transfers rotation to neighboring U and emits a **flash**. The sequence of such flashes along the P track constitutes what we observe as **light**.

2. Rotation-Based Particle Motion — Linkage Summary

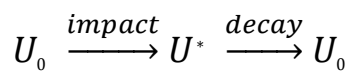
Earlier work postulated that superposed rotation fields modulate particle mobility (position/momentum distributions). ITFC instantiates this by using a **transient angular-momentum variable** ω and a **dwelt time** τ , so that an impact imparts linear impulse to P and a short-lived angular impulse to U.

3. Model Components

3.1 U- particles (unobservable background)

- **States.** Stable U_0 (non-emissive) and

excited U^* (flash-emissive). Transitions: .



- **Local dynamics.** Let ω denote transient angular speed.

$$\frac{d\omega}{dt} = \frac{\omega}{\tau} + \sum_{j \in \mathbb{N}} \kappa \omega_j \Theta(r_c - \|r - r_j\|)$$

$$I_v(t) = \eta \left| \frac{d\omega}{dt} \right|^p, \quad p \geq 1, \eta > 0.$$

3.2 P- particles (high- speed drivers)

Properties. Effectively massless energy carriers, **not directly observable**. Average speed v_p with a **lower bound** c (i.e. $v_p \geq c$). Here c is the **critical U- transfer speed** (the light constant).

Trajectory. Ballistic flight over an effective free length ℓ or transfer length λ , with direction changes upon contact according to a scattering kernel $p(\theta)$.

Contact rule. A single contact raises a local U angular speed by ω_0 and may deflect P by angle $\theta \sim p(\theta)$. **Observable propagation is governed by the U- cascade**, not by P directly.

3.3 Definition of the Cascade (Light)

Along a P track, the set U^* forms a time- ordered cascade. The detector integrates flashes over a window Δt ; the integrated signal is the **intensity**, and its stream defines a **ray**.

3.4 Observability (Afterimage Hypothesis)

P is inferred **only** via the spatio- temporal pattern of the U- cascade “afterimage”. Identical P tracks may yield different apparent rays depending on λ, τ_e .

3.5 Chain Dynamics (Summary)

U- excitation dynamics and emission follow §3.1; cascade formation is determined by $\lambda, \tau_e, \kappa, r_c$.

3.6 Parameters

λ (effective transfer length), τ_e (local dwell/lag), c (U-transfer critical speed), $p(\theta)$ (P→U scattering kernel), etc.

3.7 Summary (Causal Direction)

Cause (P) moves with $v_p \geq c \rightarrow$ **Medium (U)** undergoes transfer at **c** \rightarrow **Observation (Light)** = cascade of flashes.

4. Effective Propagation Speed and Refractive Index

The observable signal is the U- cascade. For one step,

$$t_{step} = \lambda/c + \tau_e, \quad v_{eff} = \frac{\lambda}{\lambda/c + \tau_e} = \frac{1}{c^{-1} + \tau_e/\lambda}.$$

$$n \equiv \frac{c}{v_{eff}} = 1 + \frac{c\tau_e}{\lambda}.$$

5. Optical Laws — Consequences

5.1 Rectilinearity

If scattering is forward-peaked and $\lambda \gg r_c$, deflection is small and straight-ray

propagation holds.

5.2 Reflection/Refraction (Variational Principle)

Light (the U-cascade) follows paths minimizing total time $T = \int \frac{ds}{v_{eff}(s)} = \int \frac{n(s)}{c} ds$. With

$$n(s) = 1 + \frac{c\tau_e(s)}{\lambda(s)},$$

Snell's law follows: $n_A \sin \theta_A = n_B \sin \theta_B$. Ray bending aligns with ∇n , i.e., with gradients of τ_e/λ .

5.3 Scattering and Turbidity

Stronger transport scattering shortens λ (e.g. $\lambda \approx 1/(\rho_U, \sigma_{tr})$) and typically increases τ_e by multiple contacts; hence $n = 1 + c\tau_e/\lambda$ rises and v_{eff} falls, transitioning to a transport regime characterized by an effective transport mean free path ℓ^* and diffusion coefficient $D \sim v_{eff}\ell^*/3$. Measurables: increased turbidity and delayed pulse tails.

5.4 Diffraction/Interference as Time Synchronization

Two cascades arriving within a threshold **sync time** τ_c produce fringes within the detector's integration window Δt_{int} . The **coherence length** is $L_c = v_{eff} \tau_c = \frac{c\tau_c}{1+c\tau_e/\lambda}$. Vacuum-like conditions (small τ_e/λ) yield $v_{eff} \rightarrow c$ and longer L_c , enhancing visibility; media with larger τ_e/λ reduce L_c and modulate fringe patterns.

6. Relativistic Constraints and Local Invariance

Treat c as the invariant **U-transfer critical speed**. Although $v_p \geq c$ may hold, observable information propagates with $v_{eff} \leq c$. Michelson–Morley-type nulls are recovered by **covariant scaling** of U-parameters (e.g., an invariant τ_e/λ in a local inertial frame), which removes first-order anisotropy.

7. Numerical Simulation Frame

Microscopic (agent-based): Monte-Carlo P-jumps plus U-lattice reaction-transfer $U_0 \leftrightarrow U^*$.

Continuum (PDE):

$$\partial_t u^*(r, t) = D \nabla^2 u^* - \frac{u^*}{\tau} + S_p(r, t),$$

where S_p is a source tied to P tracks.

Table 1. Model Parameters (Baseline & Sweep)

name	meaning	unit	baseline_A (vac-like)	baseline_B (dense/boundary)	sweep
ρ_U	U-particle number density	arb.	1e-3	1.0	1e-4 – 3.0
σ_{tr}	transport cross section	arb. area	1e-3	1e-1	1e-4 – 1
λ $\approx 1/(\rho_U \sigma_{tr})$	effective transfer length	arb. length	derived	derived	derived

τ_e	dwell / lag per step	time	$0.01 (\lambda/c)$	$0.3 (\lambda/c)$	$0 - 1 (\lambda/c)$
τ	decay time of excited U	time	$5\tau_e$	$2\tau_e$	$1-10\tau_e$
κ	transfer coupling strength	1/time e	$0.05/\tau_e$	$0.2/\tau_e$	$0.01 - 0.5/\tau_e$
r_c	transfer radius	length	0.5λ	0.8λ	$0.1 - 1.0\lambda$
$p(\theta)$	scattering kernel (P→U)	—	forward- peaked	broadened (near-Lambertian)	HG g: $0.9 \rightarrow 0.0$
c	U- transfer critical speed	speed	1.0 (nondim)	1.0	fixed
v_p	P speed (unobserved)	speed	$1.5c$	$1.2c$	$\geq c$
$v_{eff} = 1/(1/c + \tau_e/\lambda)$	effective propagation speed	speed	computed	computed	computed
$n = 1 + c\tau_e/\lambda$	effective refractive index	—	≈ 1.01	≈ 1.3	$1.0 - 2.0$
τ_c	sync time for interference	time	$100\tau_e$	$50\tau_e$	$10 - 200\tau_e$
$L_c = v_{eff}\tau_c$	coherence length	length	computed	computed	computed
Δt_{int}	detector integration window	time	$50\tau_e$	$50\tau_e$	$10 - 200\tau_e$
observables	$\Delta T, V, n_{eff}$	—	measure	measure	record vs sweep

Note. Start with dimensionless units and map to physical units in later experimental design. Baseline_A is vacuum- like; Baseline_B represents strong boundary/scattering conditions.

Table 2. Numerical Settings (Recommended)

item	symbol	value	note
domain length	L_{dom}	200λ	periodic or absorbing BC
grid spacing	Δx	$\lambda/20$	resolve transfer front
Time step	Δt_{num}	$0.5 \cdot \min(\lambda/c, \tau_e)$	stability / CFL- like guard
Total steps	N_{step}	1e5	cover many transfers
Particles per cell (P)	N_p	10-100	Monte- Carlo variance control
Recording cadence	—	every 50 steps	for $\Delta T, V, n_{eff}$
sources	S_p	scripted tracks	single/dual tracks for interference

Output metrics. ΔT : time delay across length L ($\int ds/v_{eff}$); V : fringe visibility $(I_{max} - I_{min})/(I_{max} + I_{min})$; n_{eff} : path- averaged refractive index $(1/L) \int n(s)ds$.

8. Experimental Predictions and Discriminators

1. Pressure/density- dependent index. Control residual gas (affecting λ, τ_e) and measure $\Delta T \sim L\Delta(\tau_e/\lambda)$.

2. Boundary dynamics. Design interfaces (metasurfaces) to tailor $p(\theta)$, inducing non- integer refraction and polarization- dependent n .

3. Time-synchronization interferometry. Scan pulse delay and locate the threshold τ_c for fringe onset.

4. UHV gas-injection step test. Micro-step λ , τ_e by controlled injections and read out femto–picosecond timing shifts via interferometry: $\Delta n \approx c\Delta(\tau_e/\lambda)$.

5. Kernel engineering at boundaries. Actively vary $p(\theta)$ and compare with ITFC predictions (cascade- transfer delays).

6. Annual/azimuthal modulation interferometry. Earth's orbit and rotation modulate the relative angle to Ω . Measure annual/diurnal components of $\Delta(\tau_{\text{swap}}/\lambda)$ as femto–picosecond delays. Scan latitude/longitude/azimuth to reject systematics and set an upper bound on $\Delta n(\Omega)$.

9. Mapping to Topological Terminology (Optional)

U- background corresponds to a near-zero phase-feedback exterior of a quasi-isolated system; contact transitions are phenomenologically analogous to entropy-direction inversions. This gives a dictionary between rotation- based/phase- based language without altering predictions.

9.1 Phase Symmetry in Nuclear Binding and Phase Relaxation (Beta Decay)

We interpret nuclear binding as a tendency to maintain **phase symmetry (or equilibrium)** within a bound system.

Let Φ_i and Φ_j denote the phases of nucleons i and j , and introduce a short-range envelope

$U(R_{ij}) \sim -J_0 \exp(-R_{ij}/\lambda_N)$. A phenomenological binding energy can be written as:

$$E_{bond} = - \sum_{\langle i,j \rangle} J_{ij}(R_{ij}) \cos(\phi_i - s_{ij} \phi_j - \pi p_{ij}) + \sum_{\langle i,j \rangle} U(R_{ij})$$

where $s_{ij} \in \{\pm 1\}$ represents the coupling sign (in-phase or anti-phase), and

$p_{ij} \in \{0,1\}$ encodes a π -junction (e.g., neutron-mediated anti-phase coupling).

Energy minimization enforces local phase equilibrium, naturally producing short-range strong attraction and saturation behavior.

In this framework, beta decay is interpreted as a **phase relaxation (phase-slip) process** that occurs when accumulated phase imbalance exceeds a critical barrier.

Introducing an isospin angle α with an effective potential:

$$U_{iso}(\alpha) = -J_{pn} \cos \alpha + \frac{K}{2} \alpha^2$$

a phase-slip transition $\alpha \rightarrow \alpha \pm \pi$ occurs when the phase energy exceeds a threshold E_b .

The released energy is partitioned as:

$$Q = \Delta E_{phase} - E_b = T_e + T_\nu + E_{U-cascade} \geq 0$$

where T_e and T_ν denote the kinetic energies of the emitted electron and (anti)neutrino,

and the remaining energy is carried by the U-cascade (flash chain).

Charge conservation is ensured via the label-charge continuity relation

(Appendix D.5')

$$\partial_t \rho_q + \nabla \cdot J_q = S_{slip}$$

which reduces to standard conservation ($S_{slip} \rightarrow 0$) in the rapid recombination limit.

Thus, beta decay is interpreted as a dynamical process restoring phase equilibrium within the bound system.

10. Limitations and Open Problems

- Establish a precise **effective field theory** mapping to Maxwell/QED.
- Quantitatively confront **high-precision null experiments**.
- Integrate a **nonlinear detector model** for biological perception.

11. Conclusion

ITFC redefines light as a **cascade of U-particle flashes** and interprets the light constant as a **U-transfer critical speed**. Thus, while a driver P may satisfy $v_p \geq c$, information transfer remains bounded by $v_{eff} \leq c$. Medium sensitivity is quantified by $n = 1 + c\tau_e/\lambda$. The frame unifies rectilinearity, reflection/refraction, scattering/turbidity, and diffraction/interference through the single spatial field τ_e/λ . We propose UHV step tests and boundary-kernel engineering as near-term discriminators.

Future work. (1) Construct a rotation- field micro- model and an EFT correspondence; (2) infer τ_e, λ from metasurface/nanointerferometry datasets; (3) precision comparisons of $\Delta T, V, n_{eff}$; (4) connect to rotation- based galactic dynamics via refractive- index mapping.

Appendix A. Covariant Parameter-Scaling Hypothesis (Sketch)

In local inertial frames, let $\lambda \propto f(\Phi)$ and $\tau_e \propto f(\Phi)$ scale homogeneously with a local scalar Φ , keeping c . Then $v_{eff}^{-1} = c^{-1} + const$ is locally invariant and first-order anisotropy cancels.

Appendix B. Notation

ρ_U : U- particle number density; σ : (transport) cross section; ℓ : transport mean free path; λ : effective transfer length; τ, τ_e : decay/dwell constants; κ : transfer coupling; r_c : transfer radius; c : U- transfer critical speed; n : effective refractive index; u^* : excited U concentration; u_p : P speed; u_{eff} : effective cascade speed.

Appendix C. Diagrams (v1)

Display note. If Mermaid is unavailable, use the ASCII alternates. Variables appear in plain text (tau_e, lambda, r_c).

[Fig. 1] U- cascade propagation (P track and excitations)

flowchart LR

P0((P)) --> U1((U*))

```

U1 --> U2((U*))
U2 --> U3((U*))
P0 -. dotted path .-> P1((P))
P1 --> U4((U*))
U4 --> U5((U*))

classDef glow fill:#ffffd6,stroke:#5555;
class U1,U2,U3,U4,U5 glow;

```

ASCII art:

```

P path: .....
          o* -> o* -> o*      (U* : excited U; flash)
            \
              -> o* -> o*

```

r_c : local transfer radius

λ : effective transfer length between successive U^*

[Fig. 2] Trajectory change at a boundary (refraction/reflection)

flowchart LR

```

subgraph A[region A:  $n_A = 1 + c \cdot \tau_{eA} / \lambda_{A}$ ]
  IA[/incident ray  $\theta_A$ /]
end

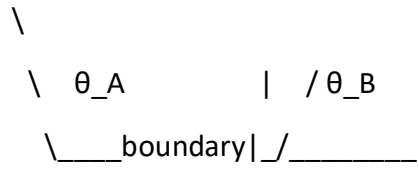
subgraph B[region B:  $n_B = 1 + c \cdot \tau_{eB} / \lambda_{B}$ ]
  RB[/refracted ray  $\theta_B$ /]
end

IA --> |boundary| RB

```

ASCII art:

region A (n_A) | region B (n_B)



Snell: $n_A \cdot \sin(\theta_A) = n_B \cdot \sin(\theta_B)$

with $n = 1 + c \cdot \tau_e / \lambda$

[Fig. 3] Time- synchronization interference (coherence length L_c)

P-chain #1: |* * * * *|

P-chain #2: |* * * * *|

<---- Δt ---->

Detector window Δt_{int} : [=====]

Sync time τ_c : threshold for fringe formation

$$L_c = v_{eff} \cdot \tau_c = c \cdot \tau_c / (1 + c \cdot \tau_e / \lambda)$$

Appendix D. Effective Action (Lagrangian) — Sketch

This appendix presents a refined **effective action** sketch for ITFC while preserving the phenomenological parameters λ , τ_e , τ_{swap} , κ . The purpose is twofold: (i) encode **memory effects** and **finite transfer range** directly in the action, and (ii) to recover, in the long- wavelength and low- frequency limit, the ITFC propagation law

$$\begin{aligned}
 t_{step} &= \frac{\lambda}{c} + \tau_{eff}, & v_{eff} \\
 &= \frac{1}{c^{-1} + \tau_{eff}/\lambda}, & n \\
 &= 1 + \frac{c\tau_{eff}}{\lambda}
 \end{aligned}$$

Where

$$\tau_{eff} = \begin{cases} \tau_e, & \text{dilute background,} \\ \tau_{swap}, & \text{dense swap – dominated background.} \end{cases}$$

D.1 Fields and External Source

Let $\psi(x) \equiv \psi(\mathbf{t}, \mathbf{r})$ denote an effective scalar field representing the **intensity/state of U-transfer**, i.e. the observable carrier of the U-cascade. The P-track enters only through an external source

$$J_p(x) = g \int d\tau \delta^{(4)}(x - X(\tau)),$$

where $X(\tau)$ is the worldline of the P-particle. Thus, P itself is not directly observable; only the induced field ψ is.

D.2 Effective Action (Sketch)

The refined effective action is written as

$$S_{eff} = \int d^4x \left[\frac{1}{2} (\partial_t \psi)^2 - \frac{c^2}{2} |\nabla \psi|^2 - V(\psi) + J_p \psi \right] + \frac{1}{2} \int d^4x d^4x' \psi(x) K(x - x') \psi(x').$$

Here $K(x - x')$ is a **causal nonlocal kernel** satisfying

$$K(t - t' < 0, r - r') = 0,$$

so that temporal ordering and observable causality are preserved.

A separable illustrative form is

$$K(x - x') = K_t(t - t') K_r(r - r'),$$

with

$$K_t(\Delta t) = \frac{\alpha}{\tau_{eff}} \exp\left(-\frac{\Delta t}{\tau_{eff}}\right) \theta(\Delta t),$$

$$K_r(\Delta r) = -\beta \frac{c}{\lambda} \frac{\exp(-|\Delta r|/\lambda)}{N_\lambda},$$

where N_λ is a normalization factor and α, β are matching coefficients.

If a cosmic reversible rotation field $\Omega = \Omega(R)$ is included, the kernel may be parameterized as

$$K(x - x'; \Omega) = K_t(t - t'; \Omega)K_r(r - r'; \Omega),$$

with Fourier transform

$$\tilde{K}(\omega, k; \Omega) \simeq A(\Omega)(i\omega) + B(\Omega)k^2 + \dots .$$

The matching conditions are then imposed as

$$\left(\frac{\partial \tilde{K}}{\partial (i\omega)} \right)_{\omega=0, k=0} = \frac{1}{\tau_{\text{swap}}(\Omega)}, \quad \left(\frac{\partial \tilde{K}}{\partial k^2} \right)_{\omega=0, k=0} = -\frac{c}{\lambda(\Omega)}$$

These ensure the long-wavelength relations

$$v_{\text{eff}}(\Omega) = \frac{1}{c^{-1} + \tau_{\text{swap}}(\Omega)/\lambda(\Omega)}, \quad n(\Omega) = 1 + \frac{c\tau_{\text{swap}}(\Omega)}{\lambda(\Omega)}$$

D.3 Equations of Motion and Dispersion (Linearized)

Near a local steady state, take

$$V(\psi) \simeq \frac{m^2}{2}\psi^2.$$

Then the Euler–Lagrange equation becomes

$$\begin{aligned} \partial_t^2 \psi - c^2 \nabla^2 \psi + m^2 \psi \\ + \int d^4 x' K(x - x') \psi(x') \\ = -J_p(x). \end{aligned}$$

For a plane-wave ansatz

$$\psi(x) \sim e^{i(k \cdot r - \omega t)},$$

one obtains the dispersion relation

$$-\omega^2 + c^2 k^2 + m^2 + \tilde{K}(\omega, k) = 0.$$

In the long- wavelength/low- frequency regime,

$$\tilde{K}(\omega, k) \approx A(i\omega) + Bk^2 + \dots ,$$

And the coefficients A and B are fixed by the ITFC matching rules below.

D.4 Long- Wavelength Matching (Design Rules)

The refined design rules are:

$$\begin{aligned} (M1) \quad t_{step} &= \frac{\lambda}{c} + \tau_{eff} \\ &\xrightarrow{\quad\quad\quad} v_{front} \\ &= \frac{1}{c^{-1} + \tau_{eff}/\lambda} \equiv v_{eff} , \end{aligned}$$

$$(M2) \quad n = \frac{c}{v_{eff}} = 1 + \frac{c \tau_{eff}}{\lambda} ,$$

$$\begin{aligned}
(C1) \quad & \left(\frac{\partial \tilde{K}}{\partial (i\omega)} \right)_0 \\
& = \frac{1}{\tau_{eff}}, \quad (C2) \quad \left(\frac{\partial \tilde{K}}{\partial k^2} \right)_0 \\
& = -\frac{c}{\lambda}.
\end{aligned}$$

Choosing α, β , and N_λ so that (C1) – (C2) hold ensures that the **front velocity** of the causal U-cascade response reproduces the ITFC law.

> **Remark.** In a generic nonlocal medium, phase velocity and group velocity need not coincide with the signal front velocity. In ITFC, the physically relevant quantity is the propagation of the **U-cascade front**.

D.5 Minimal Potential and Stability

A stable minimal potential may be chosen as

$$\begin{aligned}
V(\psi) &= \frac{m^2}{2} \psi^2 + \frac{\lambda_4}{4!} \psi^4 + \dots \\
&\cdot, \quad m^2 \geq 0, \quad \lambda_4 \geq 0.
\end{aligned}$$

If one prefers a phase interpretation, a periodic form such as

$$V(\phi) = \Lambda_\phi (1 - \cos \phi)$$

may be used instead.

D.5' Label-Charge Continuity (Noether Sketch)

Assume a global $U(1)$ -like symmetry associated with a label charge q . Then the effective current obeys

$$\partial_t \rho_q + \nabla \cdot J_q = 0.$$

D.6 Summary

The refined effective action preserves:

$$\begin{array}{ll} (1) \text{ causality,} & (2) \text{ finite memory} \\ / \text{ range } (\tau_{eff}, \lambda), & (3) \text{ invariant } c. \end{array}$$

in the long-wave-length limit. In laboratory vacuum without pair production, any effective-mass construct may be set to zero, and the pair (λ, τ_e) alone suffices. A full microscopic derivation and EFT correspondence remain future work.

References

[1] Maxwell, J. C., *A Treatise on Electricity and Magnetism*, Vols. I–II, Clarendon Press, Oxford (1873).

[2] Born, M. and Wolf, E., *Principles of Optics: Electromagnetic Theory of Propagation, Interference and Diffraction of Light*, 7th expanded ed., Cambridge University Press (1999).

- [3] Landau, L. D., Lifshitz, E. M., and Pitaevskii, L. P., **Electrodynamics of Continuous Media**, 2nd ed., Butterworth-Heinemann / Elsevier, Vol. 8 of Course of Theoretical Physics (1984).
- [4] Michelson, A. A. and Morley, E. W., "On the Relative Motion of the Earth and the Luminiferous Ether," **American Journal of Science** **34** (203), 333–345 (1887).
- [5] Feynman, R. P., **QED: The Strange Theory of Light and Matter**, Princeton University Press (1985).
- [6] Jackson, J. D., **Classical Electrodynamics**, 3rd ed., Wiley (1998).
- [7] Hecht, E., **Optics**, 5th ed., Pearson (2016).
- [8] Sakurai, J. J. and Napolitano, J., **Modern Quantum Mechanics**, 2nd ed., Cambridge University Press (2017).
- [9] Peskin, M. E. and Schroeder, D. V., **An Introduction to Quantum Field Theory**, CRC Press / Westview Press (1995).
- [10] Weinberg, S., **The Quantum Theory of Fields**, Vol. I, Cambridge University Press (1995).
- [11] Joannopoulos, J. D., Johnson, S. G., Winn, J. N., and Meade, R. D., **Photonic Crystals: Molding the Flow of Light**, 2nd ed., Princeton University Press (2008).
- [12] Ishimaru, A., **Wave Propagation and Scattering in Random Media**, Vols. I–II, Academic Press (1978).